ASDEX Upgrade Team; EUROfusion MST1 Team

Analysis of high frequency Alfvén eigenmodes observed in ASDEX Upgrade plasmas in the presence of RF-accelerated NBI ions

Published in:
Nuclear Fusion

DOI:
10.1088/1741-4326/acb831

Published: 01/04/2023

Document Version
Publisher's PDF, also known as Version of record

PAPER • **OPEN ACCESS**

Analysis of high frequency Alfvén eigenmodes observed in ASDEX Upgrade plasmas in the presence of RF-accelerated NBI ions

To cite this article: R. Ochoukov *et al* 2023 *Nucl. Fusion* **63** 046001

OPEN ACCESS
IOP Publishing | International Atomic Energy Agency
Nuclear Fusion
Nucl. Fusion **63** (2023) 046001 (8pp)
https://doi.org/10.1088/1741-4326/acb831

Analysis of high frequency Alfvén eigenmodes observed in ASDEX Upgrade plasmas in the presence of RF-accelerated NBI ions

R. Ochoukov[1,*], S. Sipilä[2], R. Bilato[1], V. Bobkov[1], M. Dreval[3], M. Weiland[1], R. Dendy[4,5], H. Faugel[1], T. Johnson[6], A. Kappatou[1], Y. Kazakov[7], K.G. McClements[5], D. Moseev[8], M. Salewski[9], P. Schneider[1], ASDEX Upgrade Team[a] and EUROfusion MST1 Team[b]

[1] Max-Planck-Institute for Plasma Physics, Boltzmannstrasse 2, 85748 Garching, Germany
[2] Department of Applied Physics, Aalto University, PO Box 14100, 00076 Aalto, Finland
[3] Institute of Plasma Physics, National Science Center 'Kharkov Institute of Physics and Technology', Kharkov, Ukraine
[4] Centre for Fusion, Space and Astrophysics, University of Warwick, Coventry CV4 7AL, United Kingdom of Great Britain and Northern Ireland
[5] CCFE, Culham Science Centre, Abingdon, Oxfordshire OX14 3DB, United Kingdom of Great Britain and Northern Ireland
[6] Fusion Plasma Physics, Department of Electric Energy Engineering, KTH, 10044 Stockholm, Sweden
[7] Laboratory for Plasma Physics, LPP-ERM/KMS, Brussels, Belgium
[8] Max Planck Institute for Plasma Physics, Wendelsteinstr. 1, 17491 Greifswald, Germany
[9] Department of Physics, Technical University of Denmark, DK-2800 Kgs. Lyngby, Denmark

E-mail: rochouko@ipp.mpg.de

Received 9 December 2022, revised 17 January 2023
Accepted for publication 2 February 2023
Published 14 February 2023

Abstract
High frequency Alfvén eigenmodes in the ion cyclotron frequency range are actively researched on the ASDEX Upgrade tokamak (AUG). The general properties of this particular mode type are: (*a*) the mode is beam-driven and, if excited, can persist for the entire duration of the beam-on time window; (*b*) the mode is sub-cyclotron with the frequency $\omega \sim 0.5\omega_{ci}$, where ω_{ci} corresponds to the on-axis cyclotron frequency of the beam ions; (*c*) the mode propagates in the counter-current/counter-injection direction; and (*d*) the field-aligned (∼toroidal) mode number is large: $|n_{//}| \sim 50$. It has been observed on AUG that radio frequency- (RF)-acceleration of beam-injected ions at the 3rd cyclotron harmonic significantly expands the number of excited modes. In this work we demonstrate how this observation is consistent with the global Alfvén eigenmode (GAE) behavior. The RF-driven fast ion population is modeled using a combination of an orbit-following Monte Carlo code (ASCOT-RFOF) and an electro-magnetic wave code (TORIC). The application of this code combination is a first to model beam-ion RF-acceleration at the 3rd cyclotron harmonic. The RF-accelerated fast ion distributions are then used to

[a] See Stroth *et al* 2022 (https://doi.org/10.1088/1741-4326/ac207f) for the ASDEX Upgrade Team.
[b] See Labit *et al* 2019 (https://doi.org/10.1088/1741-4326/ab2211) for the EUROfusion MST1 Team.
[*] Author to whom any correspondence should be addressed.

analytically calculate anisotropy-driven mode growth rates. We see that the region of positive (unstable) growth rates is expanded by RF-accelerated fast ions in both the frequency and the mode number directions for the GAEs, consistent with the measurements. Although the compressional Alfvén eigenmode growth rates are also positive for our particular fast ion distributions, the growth rate values are ~3 orders of magnitude lower. The plasma conditions on AUG are more destabilizing to the GAEs. Overall, our results are consistent with the observation of similar modes on other conventional tokamaks, namely JT-60U and DIII-D.

Keywords: Alfven eigenmodes, ICE, ASDEX Upgrade, plasma instabilities

(Some figures may appear in colour only in the online journal)

1. Introduction

Confinement and slowing down of fusion-born alpha particles play a key role in determining the efficiency of a D-T burning fusion reactor. Ideally, fast ions in magnetized plasmas slow down via Coulomb collision with bulk electrons and ions. However, under realistic conditions, high frequency instabilities can divert the fast ion energy deposition path away from the Coulomb channel [1]. Of particular concern are core localized instabilities, such as global Alfvén eigenmodes (GAEs) [2–5] and core ion cyclotron emission (ICE) [6, 7], as it is the region where the most intense fusion reactions take place. GAEs are commonly observed in neutral beam injection (NBI) heated plasmas in spherical [4, 5] and conventional tokamaks [2, 3]. These high frequency modes are sub-cyclotron, generally with frequencies ~0.5 of the fast ion cyclotron frequency value in the plasma core, and are driven by the fast ion anisotropy [3, 8, 9]. The first observation of high frequency GAEs on a conventional tokamak is attributed to DIII-D, where the mode has been initially identified as a compressional Alfvén eigenmode (CAE) [10]. More recent measurements from JT-60U [3], ASDEX Upgrade (AUG) [11, 12], and DIII-D [13] support the hypothesis that these mode are global and arise due to coupling between shear and compressional Alfvén waves. The measured frequency (ω), the parallel wavenumber ($k_{//}$), and the propagation direction match the expected GAE dispersion relation $(\omega/k_{//})^2 \leqslant {v_A}^2$, where v_A is the Alfvén speed [8, 14, 15].

It is of interest to quantify how these Alfvénic modes modify their properties in response to changes in the driving fast ion source, such as the speed and the pitch value of the fast ion driver. We have previously reported how the 3rd harmonic RF-acceleration of beam-driven fast ions has a particularly strong effect on these modes [11]. In this paper we present a detailed numerical analysis of a similar plasma scenario, now supplemented with extensive mode frequency and toroidal number measurements [12]. This analyses and measurements together provide strong support to the hypothesis that the high frequency Alfvén eigenmodes on AUG are GAEs, in agreement with similar observations from other conventional tokamaks [3, 9, 13].

2. Machine and diagnostics description

AUG is a medium-size conventional tokamak (major radius $R_o = 1.67$ m, minor radius $a = 0.5$ m) capable of operating with the on-axis toroidal magnetic field $B_o = -1.4$ to -3.0 T and $I_p = 0.4$–1.2 MA [16]. The negative magnetic field sign implies that B_o is in the counter-current direction (figure 1) but the machine can also operate in the reverse I_p/B_T configuration if needed. The tokamak is equipped with a range of auxiliary heating systems such as NBI, electron cyclotron resonance heating, and ion cyclotron range of frequencies heating (ICRF) (figure 1), which allows the machine to reach a wide range of plasma scenarios. The ICRF system is capable of operating at frequencies of 30.0, 36.5, 41.8, and 55.1 MHz, with ICRF power launched via two antenna pairs (figure 1). Hydrogen minority heating in deuterium plasma is the most common ICRF heating scheme, but the system can also run 2nd, 3rd, and 4th deuterium NBI harmonic heating scenarios as well as the 3-ion heating scheme with a He-3 minority ion. The NBI system can operate at 30–93 keV injection energies in either deuterium, hydrogen, or helium species (figures 1 and 2). The injection is done via two beam boxes, with each box containing four sources. The relevant source orientations in AUG are shown in figure 2. Note that sources 6 & 7 are directed off-axis for current drive studies.

The detection of high frequency modes in AUG plasmas is performed using an ICE diagnostic, which is a combination of B-dot probes spread out across the torus [17, 18]. For this particular study, we rely on a probe in Sector 5 and a probe array in Sector 11 (figure 1). The Sector 5 probe provides information on the emission frequency and amplitude, while the Sector 11 probe array can also measure the field-aligned (~toroidal) wavenumber $k_{//}$ of the detected wavefields [18]. The probe output voltage signals are routed via 50 Ohm coaxial cables out of the torus and are directly digitized at a sampling rate of 125 MHz, with a 14-bit 8-channel fast digitizer [12]. An in-depth description of the ICE diagnostic components and the signal analysis method can be found in our previous publications [12, 17, 18]. In the next section we will demonstrate how the AUG machine and diagnostic capabilities are used to probe high frequency Alfvén

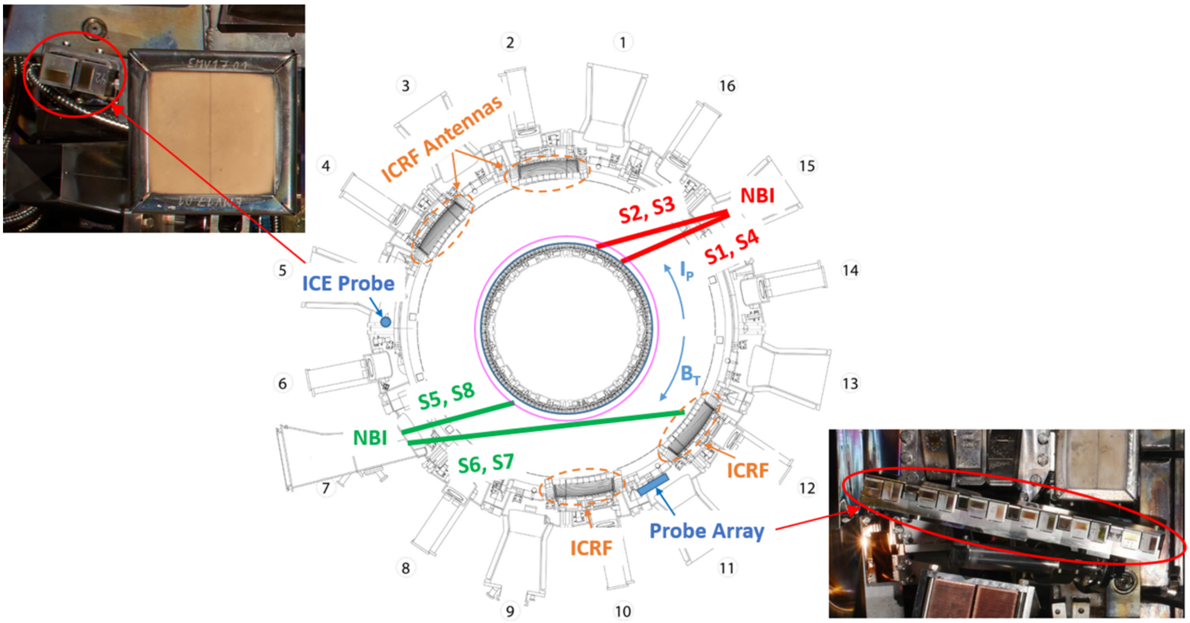

Figure 1. A top cross sectional view of AUG. Relevant heating systems and diagnostics are shown.

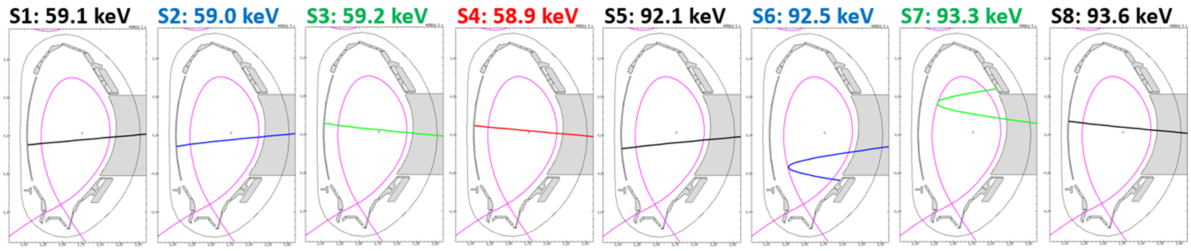

Figure 2. Poloidal NBI source orientations on AUG. The energy values refer to a typical operating value for deuterium.

eigenmode properties. These measurements are then supplemented with relevant numerical simulations to help explain observed trends.

3. Experimental results, numerical analysis and discussion

AUG is equipped with multiple NBI sources (figure 2), the voltage and the current of each individual beam being fixed during a discharge. Nevertheless, it is possible to smoothly change both the energy and the pitch angle of beam-injected fast ion populations during a discharge via RF acceleration. A particularly efficient acceleration scheme occurs at the 3rd fast ion cyclotron harmonic [19]. An example of this scheme operating in AUG is shown in figure 3. The bulk ion and the beam ion species are deuterium (with $\sim$5% H bulk concentration), with the beam ion injection energy $E_o = 93.6$ keV ($v_o = 2.99 \times 10^6$ m s^{-1}), applied for the duration of the I_p flat-top at 2.55 MW (see figure 3(*b*)). The on-axis magnetic field B_o is constant at -1.6 T, which gives the on-axis deuterium cyclotron frequency $\omega_{ci}/2\pi = 12.2$ MHz. The ICRF power (shown in figure 3(*b*)) is delivered at 36.5 MHz, which corresponds to $3 \times \omega_{ci}/2\pi$ on-axis. The ICRF power is applied in two pulses to check the reproducibility of the mode response under identical plasma conditions. There is a strong rise of the neutron rate when the ICRF power is ramped to its maximum value, shown in figure 3(*c*), which is a result of enhanced beam-target D-D fusion reactions during RF-acceleration. The frequency response of the mode to RF-acceleration of the fast ion driver contains two features, shown in figure 3(*d*). The first feature is a slight drop of the mode frequency bundle, $\sim$120 kHz or 2% of the initial frequency value $f = \omega/2\pi$, as the ICRF power is ramped up to the maximum value. This frequency drop is entirely accounted for by the rise in the core plasma electron (and the ion) density, shown in figure 3(*a*): n_e rises from 6.6×10^{19} m^{-3} to 6.8×10^{19} m^{-3}, which drops the core v_A value by 2% from 3.05×10^6 m s^{-1} to 2.99×10^6 m s^{-1}. The second feature is the appearance of additional sub-modes below the original NBI-driven mode spectra. This observation is analyzed in detail below.

The calculation of the RF-accelerated fast ion population is performed with a combination of an electro-magnetic wave code (TORIC [20]) and a particle code (ASCOT-RFOF [21]). This code combination has already demonstrated its utility at modeling hydrogen minority and second harmonic deuterium heating on AUG [21]. In this paper, we extend the codes' application to the 3rd harmonic fast deuterium

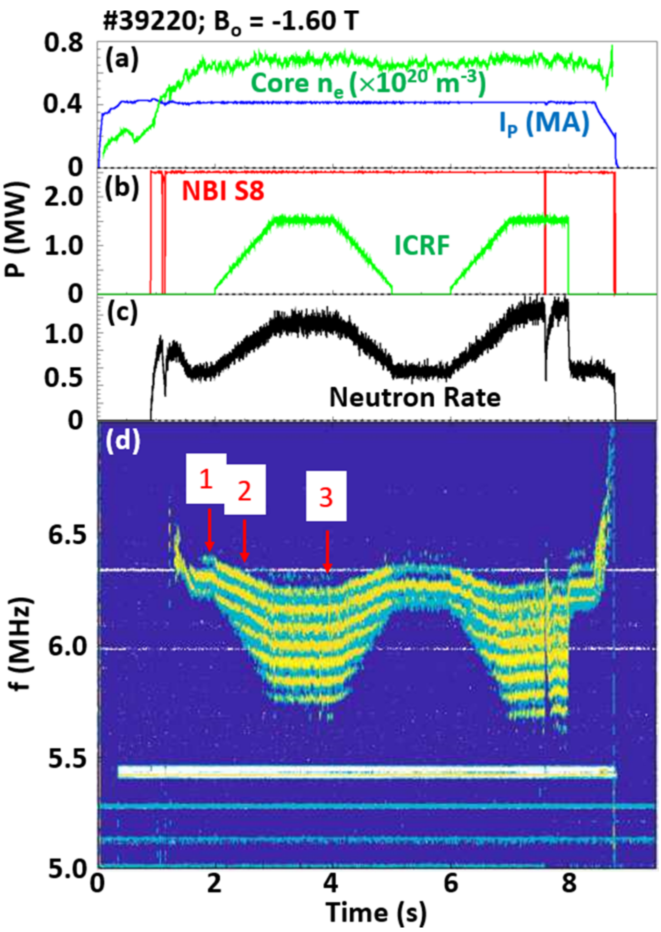

Figure 3. A 1.6 T plasma discharge example (#39220) used for analysis of a high frequency Alfvén eigenmode response to RF-accelerated NBI fast deuterium ions. (*a*) The time history of the plasma current and core plasma density. (*b*) The time history of the NBI and ICRF power. (*c*) The time history of the neutron rate. (*d*) The time history of the mode frequency spectra. The markers (1), (2), and (3) in (*d*) correspond to the time points used for ASCOT-RFOF numerical fast ion modeling (1.90, 2.50, and 3.90 s, respectively).

RF-acceleration. The modeling is performed at three time intervals, shown in figure 3(*d*): (*a*) NBI-only at 1.90 ± 0.05 s; (*b*) NBI + 1/2 ICRF power at 2.50 ± 0.05 s; and (*c*) NBI + full ICRF power at 3.90 ± 0.05 s. Only the core plasma region is used for modeling ($\rho_t < 0.2$ or $\rho_p < 0.35$, where ρ_t and ρ_p are the normalized toroidal and the poloidal flux radii, respectively). This location corresponds to the plasma region where a counter-I_p propagating GAE is localized, see for example figure 3 in Belova *et al* [9].

To improve the quantitative analysis of the simulated hot tail formation, the IC heating simulation scheme has been simplified from the one used in earlier work [21]. Instead of regenerating lost markers between time intervals of a few milliseconds, which makes scaling the results correctly more complicated, the entire ensemble of about 1.9 million markers at a time has been followed at once for the 120 millisecond simulation time, which is adequate for a steady-state hot tail to form. The scaling factor of the wave electric field components, necessary to get the correct absorbed wave power, has been determined beforehand with significantly smaller test simulations making use of RFOF's built-in E-field scaling capability. With the new simulation scheme, quantitative results of correct magnitude are obtained in a natural manner similar to pure NBI slowing-down simulations.

The first time interval (NBI-only) has been benchmarked against TRANSP [22] (see figure 4) with a good agreement between the ASCOT- and the TRANSP-modeled fast deuterium velocity distributions in the velocity (v)/trapping parameter (χ) space $f(v, \chi)$, where $\chi = (v_\perp/v)^2$ (as shown in figure 4(*c*)). The ASCOT-modeled results of the RF-accelerated population (figures 5(*d*) and (*g*), where f is normalized to the total fast ion number in the modeled volume) show the expected trend: the fast ion acceleration to higher energies (figures 5(*f*) and (*i*), RF-driven section) follows the path of higher χ. This is due to the transfer of the ICRF power primarily to the perpendicular fast ion velocity component $v_\perp$.

The calculated fast ion velocity space distributions can now be used to estimate the high frequency Alfvén eigenmode growth rate γ/ω_{ci}. This step involves an integration across a singularity and can be performed either numerically [3, 9] or analytically [8, 9]. In our manuscript, we follow the analytical approach, as derived by Lestz (equation (21) in [8]) and Belova (equation (5) in [9]). A number of approximations are used, justified by the experimental observations [11, 12]: (*a*) the measured mode frequency $\omega \sim 0.5\omega_{ci0}$; (2) the mode toroidal propagation direction is counter-I_P/counter-injection, and the toroidal mode number is very large—$n_{//} \gg 1$; 3) the mode is driven by the fast ion anisotropy in under steady-state conditions, where the inversion term $(\partial f/\partial v)$ is always stabilizing and, hence, is not included in the calculation. We reproduce equation (21) from Lestz *et al* [8] for the convenience of the reader: $\frac{\gamma}{\omega_{ci}} = \frac{\pi}{2}\frac{n_b}{n_e}\sum_l \left|\frac{v^3_{||,\mathrm{res},l}}{\omega/\omega_{ci0} - l}\right| \int \frac{xJ_l^{\mathrm{m\text{-}mode}}(\xi)}{(1-\chi)^2}\left[\left(\frac{l}{\omega/\omega_{ci0}} - 1\right)\frac{\partial f_0}{\partial \chi} + \frac{v}{2}\frac{\partial f_0}{\partial v}\right] d\chi$, where the equation parameters are defined below. The FLR (finite Larmor radius) function $J_l^{\mathrm{m\text{-}mode}}(\xi)$ for cyclotron resonance l and m-mode (=CAE or GAE) [8] is approximated in the limit $0 < \omega/\omega_{ci} < 1$ and the perpendicular wavenumber $k_\perp \to 0$, although nearly the same growth rate results are obtained in the limit $\omega/\omega_{ci} \ll 1$, with a finite $|k_\perp| \ll |k_{//}|$. ξ is the FLR parameter ($\xi = k_\perp \rho_{\perp b}$, where $\rho_{\perp b}$ is the fast ion Larmor radius), taken in the limit $\xi \ll 1$, consistent with the $|k_\perp| \ll |k_{//}|$ approximation. Net energy exchange between a mode and the fast ion population is significant only at the resonance, defined by equation (2) in Lestz *et al* [8] or equation (4) in Belova *et al* [9]. For our specific case, the resonance condition is well approximated by $\omega - k_{//}\, v_{//,\,res} = l\omega_{ci}$, where $k_{//} = n_{//}/R_o$, $R_o = 1.75$ m is the major radius position of the plasma center (where GAEs are expected to occur), $v_{//,\,\mathrm{res}}$ is the parallel beam ion velocity component in resonance with the mode, and $l = 1$ for counter-I_P propagating modes. In our approximate resonance condition equation we neglect the contribution of the toroidal bulk plasma rotation, which is about 5×10^4 m s^{-1} in the plasma core, or ∼3% of the $v_{//,\,\mathrm{res}}$ value. An example

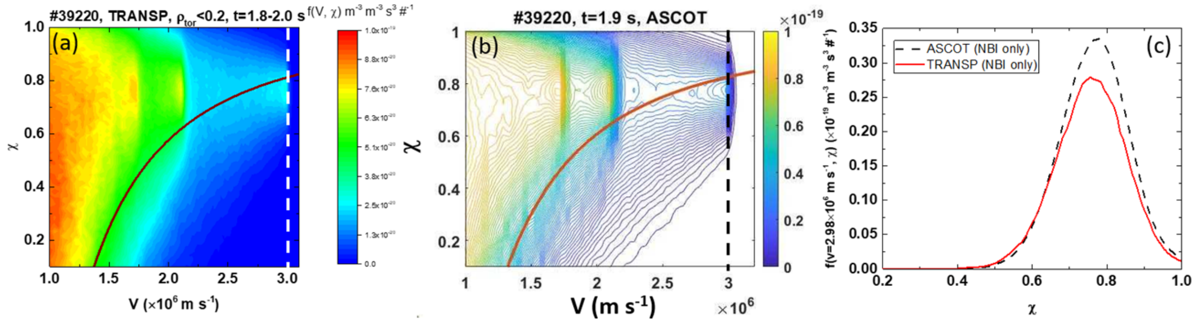

Figure 4. The fast ion distribution function generated by (*a*) TRANSP and (*b*) ASCOT-RFOF for the NBI only time frame $t = 1.9$ s. (*c*) The TRANSP and the ASCOT-RFOF generated fast ion distributions at the NBI injection speed $v = 3 \times 10^6$ m s^{-1}, see the dashed vertical lines in (*a*) and (*b*). The solid curves in (*a*) and (*b*) are resonance lines for a marginally stable mode, see figure 5 for more details.

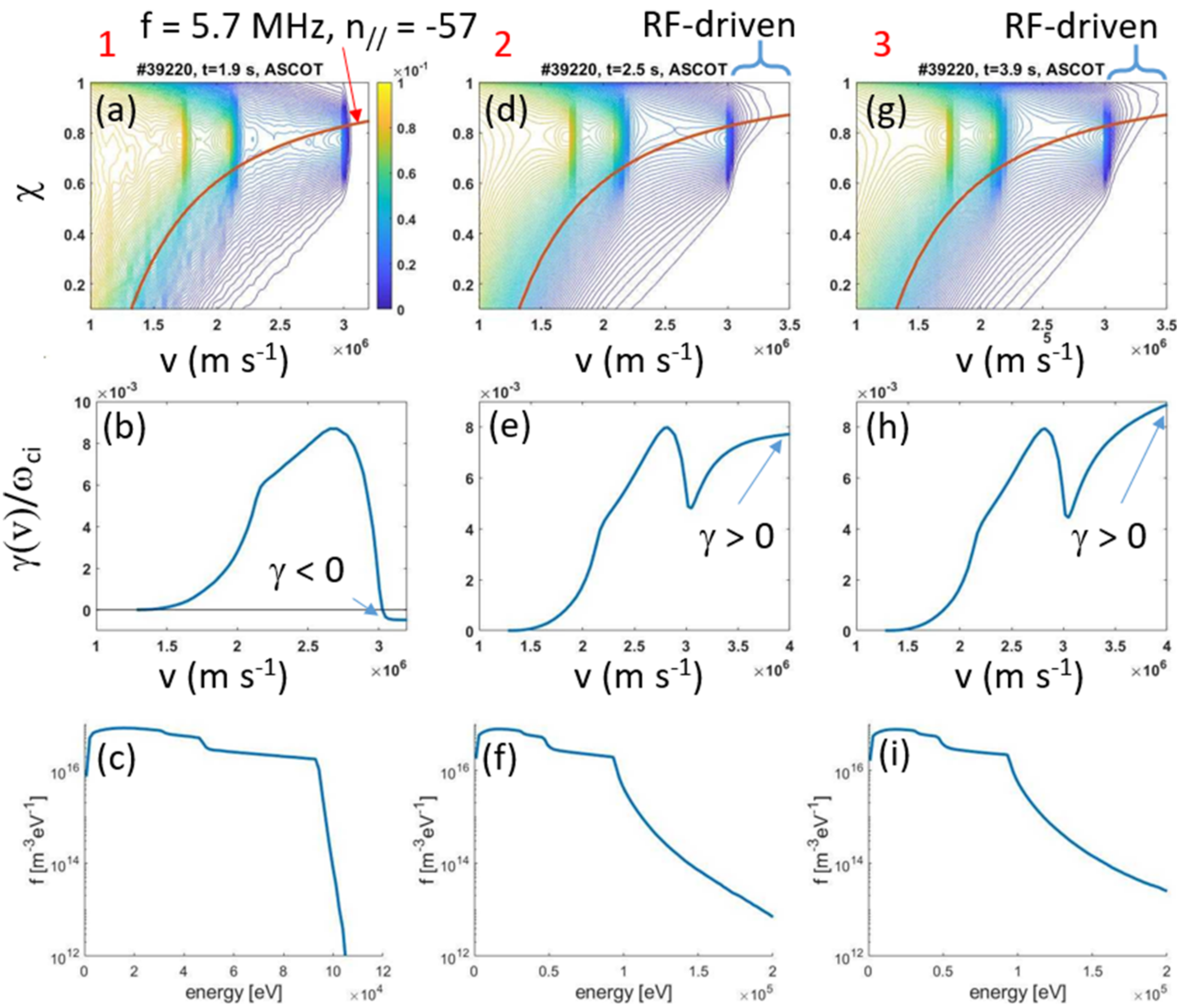

Figure 5. ASCOT-RFOF analysis results for discharge #39220. (*a*), (*d*), and (*g*) The fast ion velocity function in the v/χ space for the three time slices marked in figure 3(*d*). (*b*), (*e*), and (*h*) The GAE growth rate estimate ($\gamma(v)/\omega_{ci}$) as defined by equation (21) in [8]) for the mode example $\omega/2\pi = 5.7$ MHz and $n_{//} = -57$ for the three time slices of interest. (*c*), (*f*), and (*i*) The fast ion velocity function integrated across the trapping parameter χ for the three times slices of interest. The RF-driven fast ion component is indicated on (*d*) and (*g*) and is well-defined on (*f*) and (*i*) above 10^5 eV.

resonance curve ($\omega/2\pi = 5.7$ MHz, $-n_{//} = 57$, consistent with our measurements) is shown in figures 5(*a*), (*d*), and (*g*). This particular example demonstrates how an initially stable mode, as shown in figure 5(*b*), is destabilized by the introduction of an RF-accelerated fast ion component, as shown in figures 5(*e*) and (*h*). More specifically, it is the additional anisotropy component of the RF-accelerated fast ion population that drives more modes. In our growth rate estimates we use the beam ion fraction $n_b/n_e = 0.033$, in agreement with the experiment.

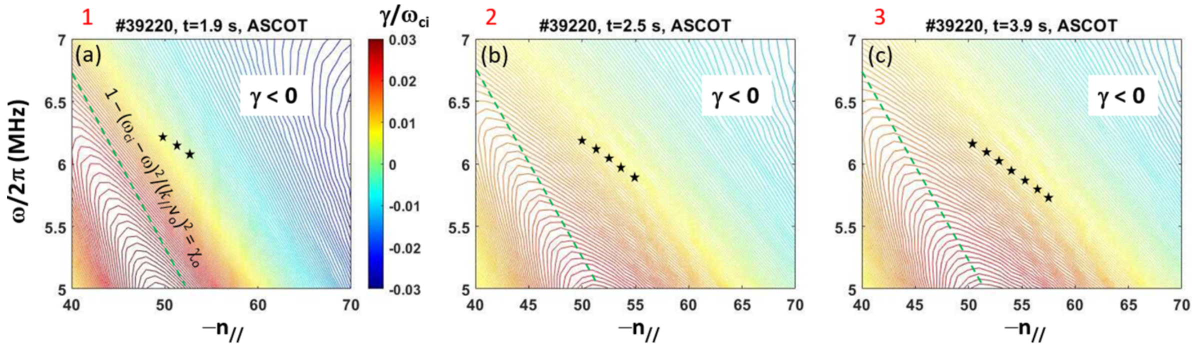

Figure 6. A 2D mode growth rate map in the frequency $\omega/2\pi$/mode number $n_{//}$ domain. (*a*)–(*c*) correspond to the times slices (1), (2), and (3) shown in figure 3(*d*), respectively. The experimental measurements are shown with star symbols. The dashed line represents the analytical estimate of the most unstable modes, as derived in [9].

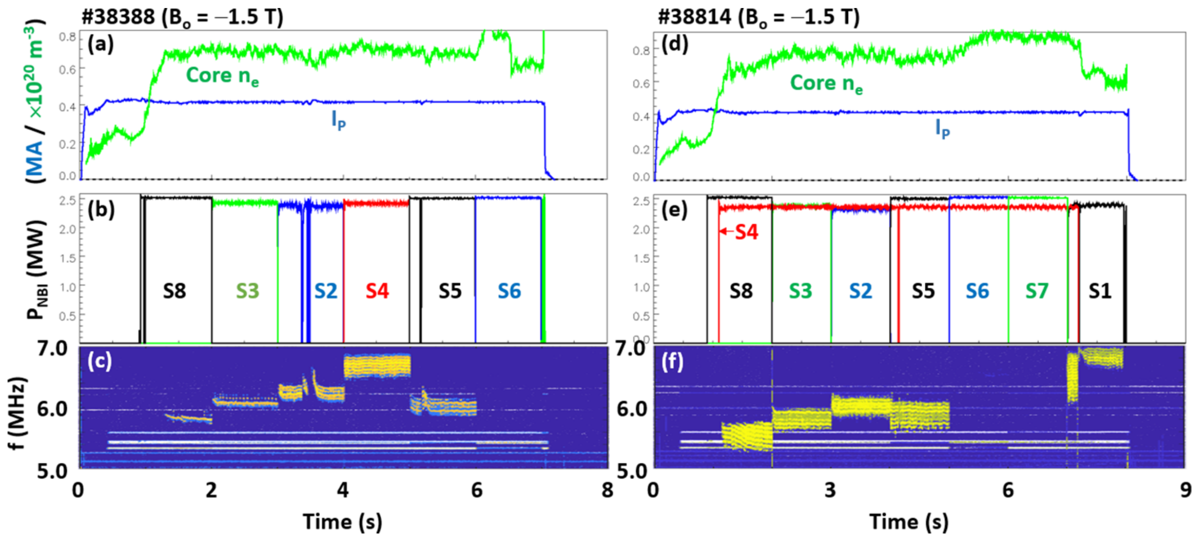

Figure 7. Two plasma discharges that demonstrate high frequency Alfvén eigenmodes driven by various NBI sources on AUG. The modes in discharge #38388 are driven by a sequence of single NBI sources, while the modes in discharge #38814 are driven by a combination of Source 4 with a sequence of the remaining sources. (*a*) and (*d*) The plasma current and the core plasma density time histories. (*b*) and (*e*) The NBI power and source time histories. (*c*) and (*f*) The mode frequency spectra time histories.

Extending the growth rate calculations to a range of frequencies and parallel mode numbers reveals a number of key features (figure 6). The peak growth rate value is expected to track the relation $1 - v_{//,\mathrm{res}}^2/v_o^2 = \chi_o$, where v_o and χ_o are the beam ion injection velocity (3×10^6 m s^{-1}) and the trapping parameter (0.78), respectively [9]. This relation is well-followed by the calculated peak growth rates, see the dashed line in figures 6(*a*)–(*c*). Additionally, we see that the RF-accelerated fast ion population expands the unstable $\omega/n_{//}$ space, as shown in the top right sections in figures 6(*b*) and (*c*). This allows for more driven modes to appear. The experimentally observed modes are shown with star symbols in figure 6. Finally, we note that performing the same growth rate calculations for counter-I_p propagating CAEs also shows a similar $\omega/n_{//}$ map of positive (unstable) values; however, the rates are three orders of magnitude lower than the GAE values. This implies that the plasma conditions in the presented discharges favor GAE emission over that of CAEs.

A more traditional way of modifying the fast ion velocity distribution in AUG plasmas is to switch between various beam ion sources (figure 2) during a single discharge. This method reveals that each NBI source on AUG has a unique mode signature in the frequency domain, ranging from 5.5 to 7.0 MHz for $B_o = -1.5$ T, as shown in figures 7(*c*) and (*f*). The general trends we observe are grouped as follows: (*a*) higher energy central sources (S5 & S8) drive modes at the lowest frequency, as shown in figure 7(*c*). This is in agreement with the condition for the existence of the resonance, defined by $\omega > \omega_{\mathrm{ci}}/(1 + v_o/v_A)$ [8, 9]. However, individual source to source variations in the mode frequency are observed (for example between S5 & S8) and suggest a hidden pitch angle dependence in the resonance existence condition. (*b*) The off-axis sources (S6 & S7) do not drive modes, but also stabilize those driven by the central sources. GAE stabilization by off-axis NBI has been observed previously on NSTX-U, a spherical tokamak, and is attributed to the reduction of anisotropy by the addition of fast ions at $\chi \to 0$. Overall, the driven mode frequency values ($\omega \sim 0.5^{*}\omega_{\mathrm{ci}}$) and plasma parameters ($v_o/v_A \sim 1$) on AUG are quite similar to the corresponding values observed on DIII-D (see figure 8 in Belova *et al* [9]). This result is not surprising, as the two machines are quite similar in size and NBI operating energy. The implication is that the two-fluid Hall correction term g must be applied to the cold plasma GAE dispersion, i.e. $\omega = gk_{//}v_{\mathrm{A}}$ with $g < 1$ [9]. Using equation (9) in Belova *et al* [9], we obtain $g \sim 0.6$ for our AUG discharges, or the expected mode frequency $\omega/2\pi = 0.6 \times 30\ \mathrm{m}^{-1} * 3 \times 10^{6}\ \mathrm{m\ s}^{-1}/2\pi = 8.6$ MHz. This estimate is within 30% of the experimentally measured 6 MHz, where the discrepancy is attributed to the scatter in the toroidal wavenumber measurement [12].

4. Summary and conclusions

The AUG tokamak is well-equipped to study electro-magnetic instabilities in the ion cyclotron frequency range. Of a particular interest are the high frequency Alfvén eigenmodes often detected on AUG [11, 12] and other tokamaks [1–5, 9, 10, 13]. The modes detected on AUG are characterized by the following properties: (*a*) the instability is beam-driven and can persist for the entire duration of the NBI-on time; (*b*) the mode frequency is generally $\sim 0.5^{*}\omega_{\mathrm{ci}}$; (*c*) the mode propagates in the counter-I_{p}/counter-injection direction; (*d*) the mode field-aligned (∼toroidal) number is large, generally ∼50. On AUG we also observe a strong increase in the mode activity in the presence of RF-accelerated beam ions, where the acceleration is at the 3rd beam ion cyclotron harmonic. In this paper we have shown that this mode response is consistent with the GAEs. The RF-accelerated beam ion distribution function has been numerically reconstructed via a combination of TORIC and ASCOT-RFOF, which is the first successful application of these codes to the 3rd harmonic acceleration. The RF-accelerated distributions have then been used to analytically calculate the anisotropy-driven GAE growth rates (figure 6) following the approach of Lestz *et al* [8] and Belova *et al* [9]. This approach shows that the unstable GAE region is expanded by the RF-driven fast ions, both in the frequency and the toroidal mode number direction, in good agreement with the measurements. The inversion-driven component ($\partial f/\partial v$) can also be included in the growth rate estimates, but it introduces only a small stabilizing effect across all frequency and mode number values without changing the overall trends shown in figure 6. Performing the same growth rate estimates for the CAEs has also shown positive (unstable) values, but these are ∼3 orders of magnitude lower. The AUG plasma properties favor the GAE emission. In summary, the GAE identity of the sub-cyclotron modes observed on AUG is consistent with the mode type detected on other conventional tokamaks, namely JT-60U [3] and DIII-D [9].

Acknowledgments

This work has been carried out within the framework of the EUROfusion Consortium, funded by the European Union via the Euratom Research and Training Programme (Grant Agreement No 101052200—EUROfusion). Views and opinions expressed are however those of the author(s) only and do not necessarily reflect those of the European Union or the European Commission. Neither the European Union nor the European Commission can be held responsible for them.

The ASCOT-RFOF simulations were carried out using the Marconi-Fusion supercomputer at CINECA, Bologna, Italy.

ORCID iDs

R. Ochoukov https://orcid.org/0000-0002-5936-113X
S. Sipilä https://orcid.org/0000-0002-2748-0601
V. Bobkov https://orcid.org/0000-0002-2328-9308
M. Dreval https://orcid.org/0000-0003-0482-0981
T. Johnson https://orcid.org/0000-0002-7142-7103
A. Kappatou https://orcid.org/0000-0003-3341-1909
Y. Kazakov https://orcid.org/0000-0001-6316-5441
K.G. McClements https://orcid.org/0000-0002-5162-509X
D. Moseev https://orcid.org/0000-0001-7955-8565
M. Salewski https://orcid.org/0000-0002-3699-679X
P. Schneider https://orcid.org/0000-0001-7257-3412

References

[1] Belova E.V., Gorelenkov N., Fredrickson E., Tritz K. and Crocker N. 2015 *Phys. Rev. Lett.* **115** 015001
[2] Tang S.X., Carter T., Crocker N., Heidbrink W., Lestz J., Pinsker R., Thome K., Van Zeeland M. and Belova E. 2021 *Phys. Rev. Lett.* **126** 155001
[3] Sumida S., Shinohara K., Ichimura M., Bando T., Bierwage A. and Ide S. 2021 *Nucl. Fusion* **61** 116036
[4] McClements K.G. and Fredrickson E.D. 2017 *Plasma Phys. Control. Fusion* **59** 053001
[5] Fredrickson E.D., Belova E.V., Gorelenkov N.N., Podestà M., Bell R.E., Crocker N.A., Diallo A. and LeBlanc B.P. 2018 *Nucl. Fusion* **58** 082022
[6] Ochoukov R. *et al* 2019 *Nucl. Fusion* **59** 086032
[7] Thome K.E., Pace D.C., Pinsker R.I., Van Zeeland M.A., Heidbrink W.W. and Austin M.E. 2019 *Nucl. Fusion* **59** 086011
[8] Lestz J.B., Gorelenkov N.N., Belova E.V., Tang S.X. and Crocker N.A. 2020 *Phys. Plasmas* **27** 022513
[9] Belova E.V., Crocker N.A., Lestz J.B. and Fredrickson E.D. 2022 *Nucl. Fusion* **62** 106016
[10] Heidbrink W.W., Fredrickson E.D., Gorelenkov N.N., Rhodes T.L. and Zeeland M.A.V. 2006 *Nucl. Fusion* **46** 324–34
[11] Ochoukov R. *et al* 2020 *Nucl. Fusion* **60** 126043
[12] Ochoukov R. *et al* 2022 *Proc. 24th RF Topical Conf.* accepted
[13] DeGrandchamp G.H., Lestz J.B., Van Zeeland M.A., Du X.D., Heidbrink W.W., Thome K.E., Crocker N.A. and Pinsker R.I. 2022 *Nucl. Fusion* **62** 106033
[14] Mahajan S.M. and Ross D.W. 1983 *Phys. Fluids* **26** 2561
[15] Belova E.V., Fredrickson E.D., Lestz J.B. and Crocker N.A. 2019 *Phys. Plasmas* **26** 092507
[16] Stroth U. *et al* 2022 *Nucl. Fusion* **62** 042006
[17] Ochoukov R., Bobkov V., Faugel H., Fünfgelder H. and Noterdaeme J.-M. 2015 *Rev. Sci. Instrum.* **86** 115112

[18] Ochoukov R. *et al* 2017 22nd topical conference on radio-frequency power in plasmas, conference proceedings *EPJ Web Conf.* **157** 03038
[19] Mantsinen M.J. *et al* 2002 *Phys. Rev. Lett.* **88** 105002
[20] Bilato R., Brambilla M., Maj O., Horton L.D., Maggi C.F. and Stober J. 2011 *Nucl. Fusion* **51** 103034
[21] Sipilä S. *et al* 2021 *Nucl. Fusion* **61** 086026
[22] Breslau J., Gorelenkova M., Poli F., Sachdev J., Pankin A., Perumpilly G., Yuan X. and Glant L. 2018 TRANSP. Computer Software (USDOE Office of Science (SC), Fusion Energy Sciences (FES) (SC-24)) (27 June 2018) (https://doi.org/10.11578/dc.20180627.4)